Universiteit Utrecht

UMC Utrecht

# The HOPS Complex is Required for Matrix Degradation through Late Endosomal Recycling of MT1-MMP

**Josette Groenhof**
**Student ID: 6298273**
**MSc Molecular and Cellular Life Sciences**

Supervisor: Jan van der Beek
First examiner: Nalan Liv
Second examiner: Antoine Khalil
Research group: Klumperman Group, UMC Utrecht

UMC Utrecht,
Boelelaan 100, Utrecht
10-06-2022

# Table of Contents

# Abstract

MT1-MMP is a type I transmembrane proteinase that plays a key role in cancer metastasis through degradation of the extracellular matrix (ECM) and activation of other proteases. Recycling of MT1-MMP is essential for its function in cellular invasion. During its recycling, the HOPS complex is involved in late endosomal trafficking of MT1-MMP. Here, we investigate the role of HOPS in recycling of MT1-MMP in more detail. Depletion of HOPS subunits VPS18 and VPS39 results in accumulation of MT1-MMP in mixed endolysosomal compartments. Migration assays of these lines revealed that cell motility in 2D was unaffected. However, cell motility in 3D, for which ECM degradation is crucial, was significantly decreased in the VPS39 knockouts. Further analysis of the degradative capacity in a gelatin degradation assay revealed that knockout of VPS18 and, more strongly, VPS39 inhibits matrix degradation. By total internal reflection microscopy (TIRF) of MT1-MMP exocytic events, we describe impaired lysosomal trafficking in the HOPS knockouts. We demonstrate that MT1-MMP mislocalises and its trafficking is impaired upon depletion of the HOPS complex. Furthermore, the HOPS complex and VPS39 specifically are required for ECM degradation and invasion. Taken together, this indicates an indispensable role for HOPS in recycling of MT1-MMP and cancer cell invasion.

# Layman’s Summary

The main cause of death in cancer patients is the formation of secondary tumours. This happens through a process called metastasis, wherein cancer cells spread throughout the body. To do this, cancer cells need to migrate through the extra cellular matrix, a thick structure that supports the cells. This process involves degradation of the extracellular matrix by proteins called Matrix Metalloproteinases. MT1-MMP is one of these proteins and it has many downstream effects that facilitate matrix degradation. Recycling of this protein is indispensable for its function in degradation. The HOPS complex is a protein complex that has been found to play a role in the recycling of MT1-MMP. In this research, we show that deletion (knockout) of HOPS subunits VPS18 and VPS39 causes accumulation of MT1-MMP in the recycling pathway. Migration assays of these cells reveal that cell motility in 2D is unaffected by knockout of VPS18 or VPS39. However, cell motility in a 3D gel, for which matrix degradation is crucial, was significantly decreased in cells with VSP39 knockout. A gelatin degradation assay showed that the VPS39 knockout cells could not degrade gelatin as well as other cells. This means that knockout of VPS39 results in decreased degradation capacity. In conclusion, the HOPS complex plays an essential role in recycling of MT1-MMP, which is a crucial process in cancer metastasis.

# Introduction

Cancer is a leading cause of death worldwide (*Cancer*, 2022, Ferlay et al., 2014). Though the disease has many different genotypes, the main cause of death in patients is the development of metastasis (Sporn, 1996, Seyfried & Huysentruyt, 2013). In metastasis, cancer cells break away from the primary tumour and enter the bloodstream or lymphatic system, spreading to different parts of the body where they form secondary tumours (Geiger & Peeper, 2009). Cell migration is a crucial process during tissue development, wound healing and immune responses, but tumour cells exploit this mechanism when they metastasise. The process of metastasis is thoroughly investigated and three main steps have been identified: upregulation of contractile forces and cytoskeletal dynamics, increased turnover of adhesion molecules and formation of specialised degradative cell structures (Gimona et al., 2008).

To metastasise, cells have to breach the basal membrane and then penetrate the stiff, highly cross-linked extracellular matrix (ECM) (Stetler-Stevenson et al., 1993, Mignatti & Rifkin, 1993, Nakahara et al., 1997, Hanahan & Weinberg, 2000). The ECM provides structural support, maintains tissue connectivity and functions in cellular differentiation and homeostasis (Hynes, 2009, Frantz et al., 2010). The ECM consists of glycosaminoglycans and proteoglycans that form a thick hydrated gel. This gel is stabilised by fibrous proteins like fibronectins, laminins, elastins and collagens that form an interconnected network (Alberts, 2017). Of these proteins, collagens are the most abundant, making up as much as 30% of the total protein mass in animals (Ricard-Blum, 2010). Their main function is to provide structural stiffness and to guide tissue regeneration through regulation of cell adhesion and migration (Rozario & DeSimone, 2010, Lodish et al., 2016, Nicolas et al., 2020). The cross-linked nature of collagens favours proteolytic mechanisms of invasion, where the ECM is locally degraded through hydrolytic cleavage by secreted proteases. However, other evidence suggests a protease-independent mechanism where cancer cells use actomyosin-based structures to displace the ECM physically, after which they adopt an amoeboid morphology to propagate further into the matrix (Friedl & Wolf, 2003, Wyckoff et al., 2006, Wolf et al., 2007). These *in vitro* studies have been challenged by findings that non-proteolytic mechanisms of invasion are only possible in matrices with low levels of cross-linking, not in densely cross-linked *in vivo* tissues (Hotary et al., 2003, Sabeh et al., 2004, 2009, Wolf et al., 2013). Taken together, proteolytic ECM remodelling undoubtedly plays an indispensable role in cellular invasion through high-density tissues where cell deformability alone is not sufficient for penetration.

**Invadopodia and MT1-MMP**

Remodelling of the ECM in metastasis occurs via specific matrix-degrading protrusions, known as invadopodia (Stetler-Stevenson et al., 1993, Mignatti & Rifkin, 1993). These F-actin-rich structures facilitate local secretion of proteases, such as serine proteinases, cathepsin proteinases, ADAMs (a disintegrin and metalloproteinase) and matrix metalloproteinases (MMPs), all of which are indicative of poor patient prognosis when upregulated (Linder et al., 2011, Tanabe & List, 2016, Olson & Joyce, 2015, Carl-McGrath et al., 2005, Redondo-Muñoz et al., 2006, Sounni et al., 2002). The MMPs in particular play a key role in matrix degradation (Egeblad & Werb, 2002, Kessenbrock et al., 2015). Of the 28 identified members of the superfamily, membrane type-1 metalloproteinase (MT1-MMP or MMP-14) is investigated most intensively because of its multiple roles in degrading the ECM. It has proteolytic activity towards several ECM components (e.g. collagen I, II, III, gelatin and laminins 1 and 5, Hotary et al., 2003, D'ortho et al., 1997, Ohuchi et al., 1997, Koshikawa et al.,

2000) and activates other MMPs, such as proMMP-2 and proMMP-13 (Sato et al., 1994, Knäuper et al., 1996, Seiki et al., 2003). Moreover, MT1-MMP regulates intracellular signalling in tumour growth (Knapinska & Fields, 2019). Live-cell imaging shows that recruitment of MT1-MMP to invadopodia is quickly followed by ECM degradation (Artym et al., 2006) and *in vivo* findings report that silencing of MT1-MMP impairs invasion (Lu et al., 2010, Lodillinsky et al., 2015). This further emphasises the role of MT1-MMP in metastasis.

To degrade the ECM, MT1-MMP must be localised to the invadopodial membrane (Nakahara et al., 1997). However, it can be inactivated by autoproteolytic cleavage (Lehti et al., 2000) or interactions with RECK (reversion-inducing-cysteine-rich protein with Kazal motifs) (Oh et al., 2001, Meng et al., 2008) and TIMP (tissue inhibitor of metalloproteinases) 2, 3 and 4 (Will et al., 1996, Bigg et al., 2001). Inactivation can be reversed after endocytosis, which necessitates a high turnover rate wherein endocytosis and recycling play essential roles (Itoh & Seiki, 2004). MT1-MMP is endocytosed through clathrin- and caveolae-mediated pathways (Remacle et al., 2003, Gálvez et al., 2004). Silencing of Endophilin A2, a protein required for scission of clathrin-independent vesicles, impaired MT1-MMP internalisation and ECM breakdown (Baldassarre et al., 2015). This was attributed to a decrease in internal MT1-MMP reserves. The importance of this internal pool for recycling is highlighted by earlier data of Hoshino et al. (2012), who reported very rapid recovery of MT1-MMP at invadopodia after FRAP (Fluorescence Recovery after Photobleaching) because of this pool. Interestingly, inhibition of MT1-MMP recycling leads to higher levels of surface bound MT1-MMP and simultaneously impairs invasion (Uekita et al., 2001, Williams & Coppolino, 2011), highlighting endocytic recycling as a key step in MT1-MMP-dependent ECM degradation.

**MT1-MMP Recycling Pathways**

After endocytosis, MT1-MMP is transported to early endosomes (EE, Figure 1. I), where it colocalises with EEA1 (Early Endosome Antigen1) and the GTPase Rab5 (Remacle et al., 2003, Williams & Coppolino, 2011, Linder & Scita, 2015). From this compartment, proteins are recycled back to the plasma membrane via recycling endosomes that are Rab11 positive (Ullrich et al., 1996), or they remain in the early endosome, which matures into a late endosome (Figure 1. II). The maturation of early endosomes into late endosomes is marked by a quick transition from Rab5 to Rab7 GTPase markers (Rink et al., 2005, Poteryaev et al., 2010). MT1-MMP was found to colocalise with late endosomal markers Rab7 and VAMP7 (vesicle-associated membrane protein 7), but not Rab11 (Williams & Coppolino, 2011), indicating that it is recycled via late endosomes (Yu et al., 2012, Macpherson et al., 2014). VAMP7, a SNARE protein that plays a role in late endosomal fusion events (Pryor et al., 2004), colocalised with MT1-MMP at proteolytic sites as well, and its ablation decreased the amount of invadopodia, as well as MT1-MMP-dependent degradation (Steffen et al., 2008). This is in line with findings by Williams & Coppolino (2011), who reported disruption of MT1-MMP recycling and decreased invasion upon expression of dominant negative forms of Rab7 and VAMP7. Molecularly, VAMP7 forms a complex with Syntaxin4 and SNAP23, targeting MT1-MMP to invadopodia and inducing membrane fusion between late endosomes and the plasma membrane via their SNARE properties (soluble *N*-ethylmaleimide-sensitive factor-activating protein receptor, Williams et al., 2014). This mechanism could play a role in MT1-MMP recycling pathways through direct fusion of late endosomes with the plasma membrane (Figure 1. III C, Hakulinen et al., 2008), and/or fusion of small late endosome derived vesicles with the plasma membrane (Figure 1. III A, Rossé et al., 2014, Huotari & Helenius, 2011).

An alternative recycling mechanism is through the formation of a tubular structure between late endosomes and the plasma membrane (Figure 1. III B). Monteiro et al., (2013) observed focal delivery of MT1-MMP through thin cylindrical shapes between the late endosome and the plasma membrane that were positive for Wiskott-Aldrich syndrome protein and Scar homolog (WASH) and the exocyst complex, which plays a role in the tethering of exocytic vesicles to the plasma membrane (Liu et al., 2009). WASH interacts with actin nucleator ARP2/3, a protein involved in a signalling cascade required for the formation of invadopodia (Oser et al., 2009, Derivery et al., 2009, Yamaguchi et al., 2005). Furthermore, WASH recruits JNK-interacting protein 3 and 4 (JIP3 and JIP4), that in turn can bind both kinesin-1 and dynactin-dynein on MT1-MMP positive endosomes (Marchesin et al., 2015). The switch between these motor proteins is regulated by the GTPase ARF6, that opposes dynactin-dynein movement and promotes tubulation by kinesin-1, allowing MT1-MMP to transport to the plasma membrane. WASH itself has been found to be recruited to Rab7 positive endosomes by the Retromer complex and the sorting nexin SNX27, that are also both direct interactors of MT1-MMP (Seaman et al., 2013, Temkin et al., 2011, Sharma et al., 2019). While Retromer has been shown to play a central role in plasma membrane recycling or various cargoes (Burd & Cullen, 2014), sorting nexins have been established as the cargo-specific regulators of tubular-based endosomal sorting (Cullen, 2008). In summary, MT1-MMP can be recycled using multiple pathways, but its targeting to late endosomes is a crucial step in this process.

**HOPS in MT1-MMP Recycling**

Recently, the HOPS complex (homotypic fusion and vacuole protein sorting complex) was implicated in late endosomal MT1-MMP trafficking (Kajiho et al., 2016). The HOPS complex is a multi-subunit tethering complex that regulates tethering and fusion among late endosomes and lysosomes, as well as autophagosomes and lysosomes (Pols et al., 2013). It consists of six subunits; four are shared with the early endosome tethering complex CORVET, VPS11, VPS16, VPS18 and the SNARE-interacting VPS33A. The remaining two, VPS39 and VPS41, are HOPS specific. (Balderhaar & Ungermann, 2013, Bröcker et al., 2012). While VPS39 and VPS41 bind Rab7, CORVET specific subunits bind Rab5 (Plemel et al., 2011, van der Kant et al., 2015). This mechanism guarantees specific membrane fusion of distinct endosomal compartments (Solinger & Spang, 2013). On late endosomes, HOPS governs fusion in conjunction with a SNARE complex consisting of Syntaxin7, Vti1b, Syntaxin8 and VAMP8 for homotypic fusion, and VAMP7 instead of VAMP8 to mediate heterotypic fusion (Pryor et al., 2004, Luzio et al., 2009). It is clear that HOPS plays a crucial role in the coordination of endosomal trafficking. However, as subunits are shared between HOPS and CORVET and individual subunits have their own distinct functions (Pols et al., 2013, Jonker et al., 2018, Segala et al., 2019), analysis of the specific role of HOPS in recycling of MT1-MMP is challenging.

Taken together, it is clear that the endolysosomal system plays an important role in the metastatic capacity of tumour cells. This underlines the relevance of a deeper understanding of the recycling and trafficking mechanisms involved in tumour invasion. Here, we investigate the role of the HOPS complex in the recycling of MT1-MMP. Specifically, at which stage in endo-lysosomal trafficking HOPS is required and whether this is of functional importance for cell ECM invasion. Using immunofluorescence and electron microscopy, we assessed the effect of knocking out HOPS subunits VPS18 and VPS39 on MT1-MMP localisation. We found accumulation of MT1-MMP on

hybrid endosomal compartments, indicating deregulation of endosomal maturation. Impaired degradative capacity and cell motility through collagen I matrix reveal the functional consequences of HOPS depletion. We propose that HOPS depletion impairs recycling of proteolytic enzymes, such as MT1-MMP, from late endosomal compartments, which leads to decreased metastatic capacity.

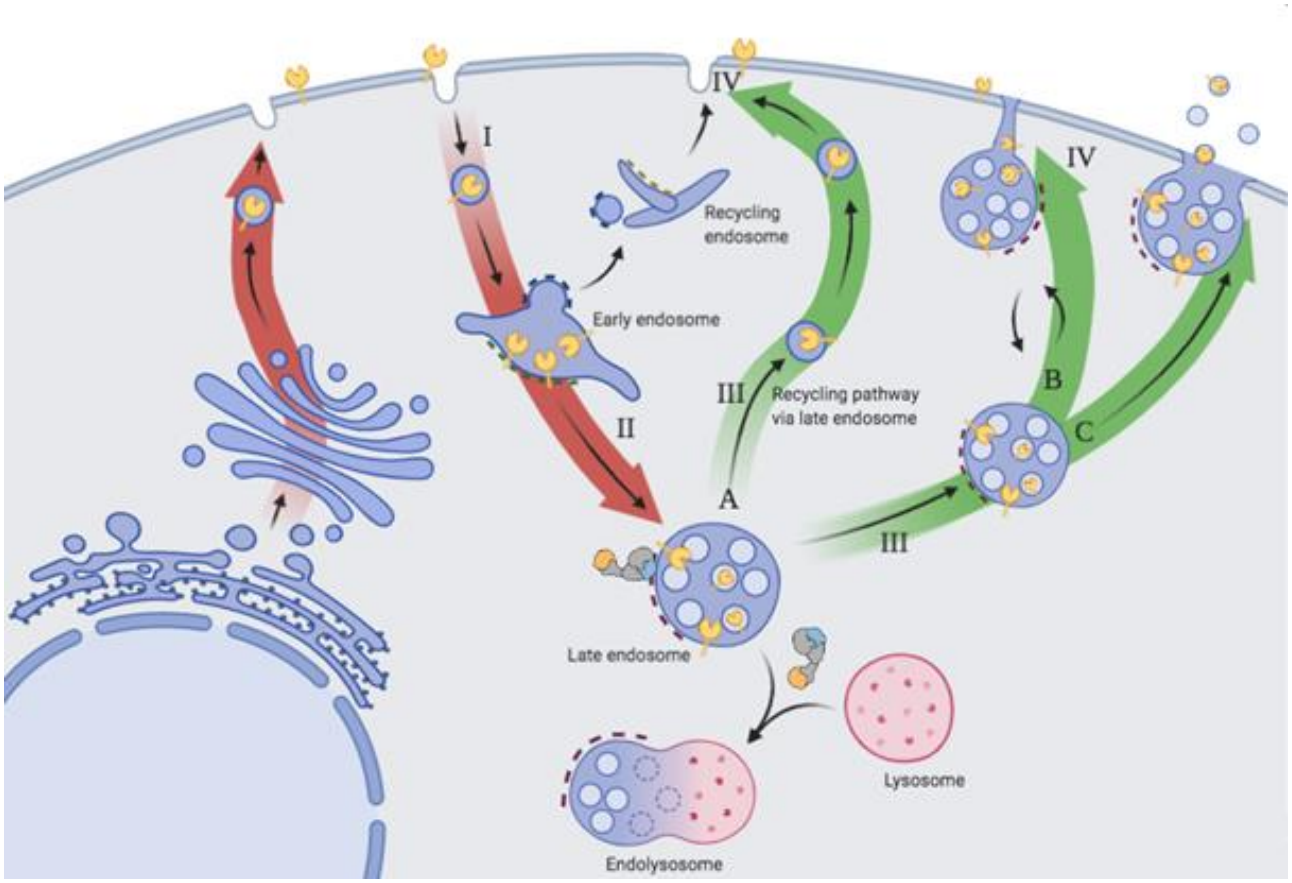


**Figure 1. Recycling pathways of MT1-MMP.** After transcription, MT1-MMP is recycled to the plasma membrane form where it endocytosed (I). Instead of being directly recycled with recycling endosomes, MT1-MMP is likely trafficked to late endosomes (II). From here on out, MT1-MMP can be recycled back to the plasma membrane (III). This may involve trafficking with small late endosome derived vesicles (A), a tubular connection between the late endosome and the plasma membrane (B) or direct fusion of the late endosome with the plasma membrane (C). Adapted from “HOPS is involved in the recycling of MT1-MMP from late endosomes to the invadopodial plasma membrane” by Kamphuis, L. M. (2020). [Unpublished manuscript].

# Results

## MT1-MMP localises to hybrid early and late endosomal compartments

As a first step in understanding the role of the HOPS complex in endosomal MT1-MMP trafficking, we sought to investigate the effect of HOPS depletion on the cellular localisation of MT1-MMP. HT1080 is a fibrosarcoma cell line often used as a model for cell invasion and migration research. In previous studies, we successfully generated HT1080 VPS18 and VPS39 knock out (KO) cell lines (Kamphuis, 2020). We found that the distribution of MT1-MMP in these HOPS KOs was altered: there were more distinct intracellular puncta, compared to a more diffuse distribution in WT cells. In order to find out to what compartments MT1-MMP localises, we performed immunostaining of MT1-MMP, early endosomal marker EEA1 and lysosomal protease Cathepsin D (Figure 2A). VPS18 and VPS39 KOs did not reveal an altered localisation of MT1-MMP in early endosomes (Sup. 1A), but we observed a significant increase in colocalisation of MT1-MMP with Cathepsin D (Figure 2B). This indicates MT1-MMP localises to both early endosomes and lysosomes in the KOs. We performed additional immunofluorescence of lysosomal-associated membrane protein 1 (LAMP1) with a GFP variant of MT1-MMP (MT1-MMP-pHluorin) and found that the KOs exhibited more colocalisation with LAMP-1 (Figure 2C). These results indicate mislocalisation of MT1-MMP to late endosomes or lysosomes in HOPS KO cells.

To localise MT1-MMP in ultrastructural context, we performed electron microscopy (EM). We prepared HT1080 cells stably expressing MT1-MMP tagged with GFP variant pHluorin for immunogold labelling. After gelatin embedding and cryosectioning, we labelled for GFP (Figure 2D). This revealed MT1-MMP mostly bound to small endosomes and vesicles in HT1080 WT cells. In VPS39KO cells, MT1-MMP was mainly found in multivesicular bodies (MVBs) with hybrid early and late endosomal morphology. This indicates that depletion of HOPS results in hybrid endolysosomal compartments. Additionally, MT1-MMP localises to these compartments, unable to traffic from the late endosomal stage.

To see whether this altered localisation has an effect on cellular morphology, we labelled cells for the focal adhesion protein Paxillin, as well as actin and MT1-MMP (Figure 3). We were unable to detect colocalisation of MT1-MMP with Paxillin, and colocalisation with actin was comparable for all cell lines (Sup. 1B). However, we observed more distinct Paxillin positive streaks in wildtype cells than in the HOPS KOs, indicating that the formation of focal adhesions might be impaired in these lines. This suggests that HOPS depletion could have functional consequences for cellular adhesion and migration.

## HOPS depletion decreases degradation-dependent cell motility

Given the increased late endosomal localisation of MT1-MMP and the reduction in focal adhesions, we sought to investigate if HOPS depletion has functional consequences on cell migration. Migration in 2D involves modulation of the cytoskeleton, cell adhesions, and protein recycling, but it does not require ECM degradation. Therefore, we can establish the effect of HOPS depletion on degradation-independent mechanisms of cell migration in a 2D migration assay. We generated cell lines stably expressing the nuclear protein H2B-mNeonGreen for accurate tracking of cell movement. Then, we performed overnight life cell imaging of these lines seeded on coverslips coated with a thin layer of collagen I (Figure 4A). Through tracking of the cell nuclei, we found

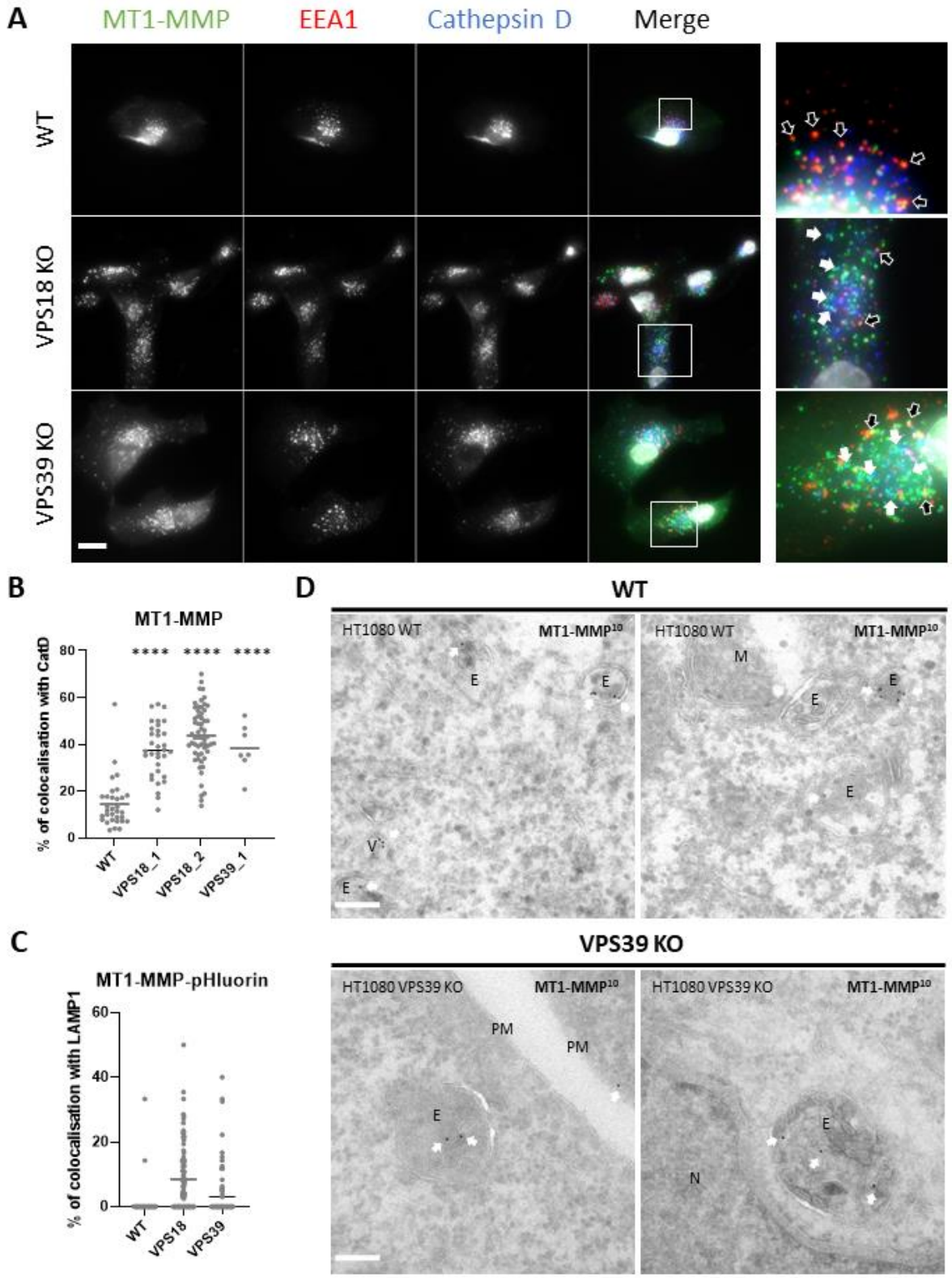


**Figure 2. MT1-MMP localises to mixed compartments in HOPS depleted cell lines. A.** HT1080 wildtype, VPS18 KO and VPS39 KO cells were immunostained for MT1-MMP (green), EEA1 (red), Cathepsin D (blue) and with DAPI (white). Black arrows indicate MT1-MMP and EEA1 positive puncta, while white arrows indicate MT1-MMP and Cathepsin D positive puncta. Scalebar 20 µm. **B.** Quantification of the colocalisation of MT1-MMP and Cathepsin D. Unpaired t-test, VPS18_1 ($p < 0.0001$, ****), VPS18_2 ($p < 0.0001$, ****), VPS39_1 ($p < 0.0001$, ****). **C.** Quantification of the colocalisation of MT1-MMP GFP variant MT1-MMP-pHluorin and LAMP1. Unpaired t-test, VPS18 ($p < 0.0001$, ****), VPS39 ($p = 0.0006$, ***). **D.** Immuno-electron microscopy of MT1-MMP (white arrows) in WT shows accumulation in vesicles (V) and endosomes (E), (M = mitochondria, PM = plasma membrane, N = nucleus). VPS39 KO lines exhibit accumulation in mixed endosomal compartments. Scalebar 200 nm.

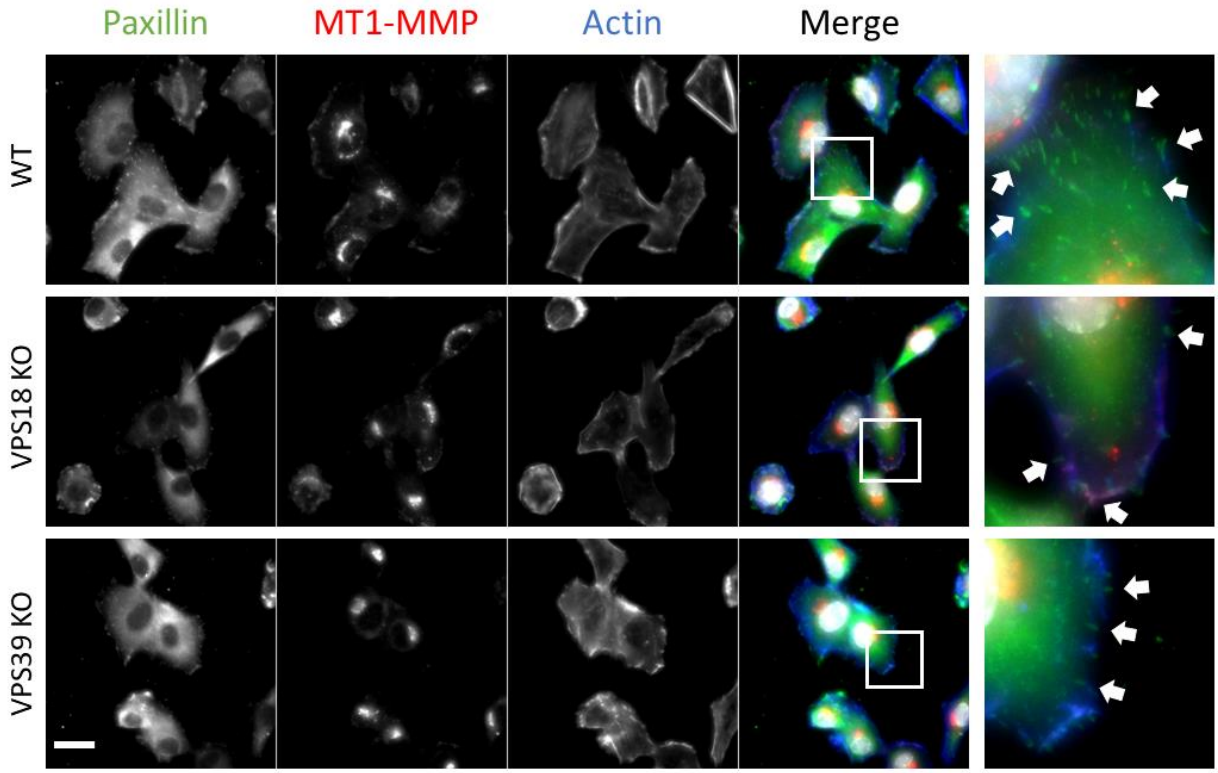


**Figure 3. HOPS depletion impairs formation of focal adhesions.** Cells were stained for Paxillin (green), MT1-MMP (red), with phalloidin for actin (blue) and DAPI (white). Wildtype exhibits profound formation of focal adhesions (white arrows), while HOPS KO cell lines show a reduced amount of Paxillin positive streaks. Scalebar 20 µm.

comparable track lengths for all cell lines (Figure 4B, Sup. 2). From these experiments, we can conclude that HOPS depletion does not interfere with cellular systems required for 2D migration.

We followed up by investigating the requirement of HOPS in a more physiologically relevant system. By seeding cells in a gel of polymerized collagen I, we assessed the effect of HOPS depletion on cell motility. Due to the tightly cross-linked bundles of collagen I in the gel, cells need to break down collagen I to move directionally. Therefore, track length in a 3D cell culture is, in part, a readout for the degradative capacity of a cell line. We seeded H2B-mNeonGreen expressing cells in a collagen I gel, incubated overnight and then imaged cellular movement (Figure 4C, D). The VPS18 KO clones showed more variability in their track length, with averages similar to or slightly higher than WT cells. KO of VPS39 significantly decreased the track length of cells, evident of reduced ability to migrate through collagen I matrix. Given that non-degradative aspects of migration were unaltered in the 2D migration assay, this result is indicative of a decreased ability to degrade collagen I, which is consistent with an effect on MT1-MMP trafficking.

## ECM degradation is impaired in HOPS depleted cell lines

To examine the effect of HOPS depletion on ECM degradation further, we performed a gelatin degradation assay. Cells were seeded on fluorescently labelled gelatin and incubated for three hours, allowing the cells to degrade the gelatin. The coverslips were then fixed and stained for actin and DAPI (Figure 5A). WT cells seeded in presence of MMP inhibitor GM6001 functioned as a

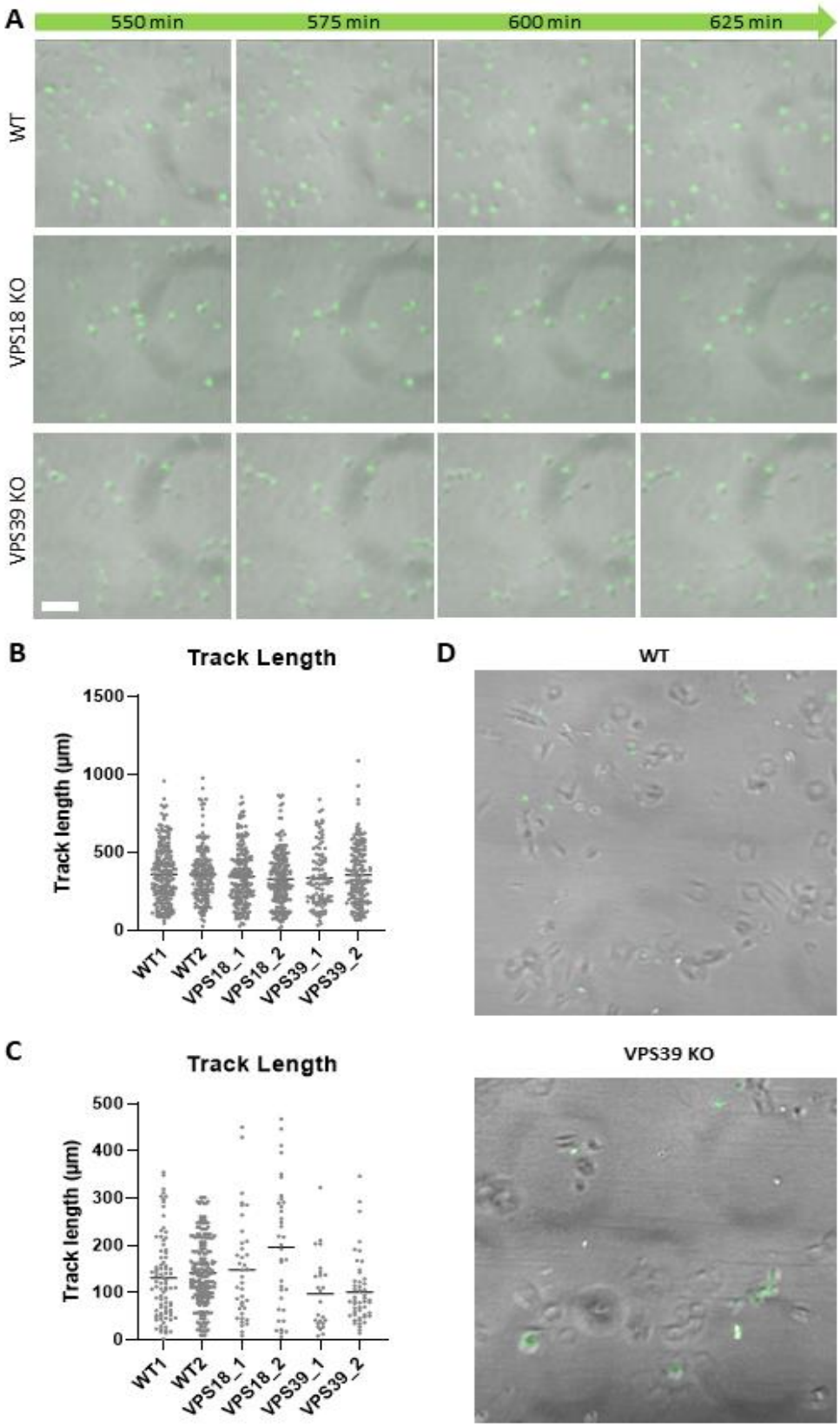


**Figure 4. Cell motility dependent on ECM degradation is decreased in HOPS depleted cells. A.** Stable cell lines expressing H2B-mNeonGreen were seeded on collagen I-coated coverslips for 2D life cell imaging overnight (14h) and results were analysed in Imaris. Scalebar 200 µm. **B.** Analysis with Imaris yielded the quantification of cellular track lengths in the 2D migration assay (n > 50). One-way ANOVA, p = 0.5193, ns. **C.** Stable H2B-mNeonGreen expressing cell lines were seeded in a 3D collagen I gel and imaged overnight (14h). Analysis with Imaris yielded the quantification of cellular track lengths in the 3D migration assay (n > 20). Unpaired t-test, VPS18_1 (p = 0.6189, ns), VPS18_2 (p = 0.003, ***), VPS39_1 (p = 0.0042, **), VPS39_2 (p = 0.003, ***). **D.** Visualisation of the H2B-mNeonGreen cells in the 3D collagen I gel.

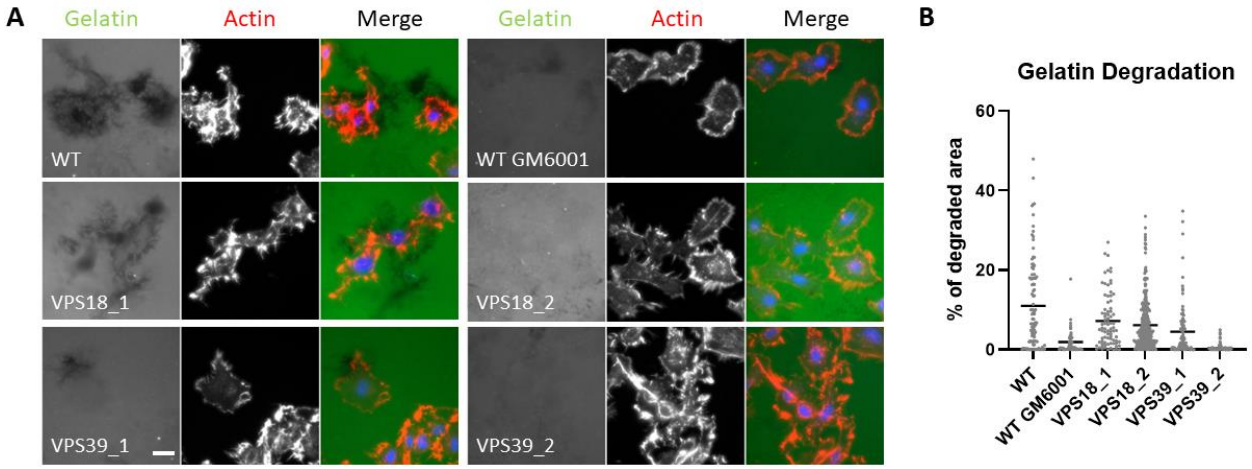


**Figure 5. HOPS depletion impairs gelatin degradation. A.** Cells were seeded on coverslips coated with fluorescently labelled gelatin (green) and incubated for 3h, then they were fixated and stained with DAPI (blue) and phalloidin for actin (red). Scalebar 20 µm. **B.** Quantification of the total percentage of degraded area under each cell (n > 50). Unpaired t-test, VPS18_1 (p = 0.0082, ***), VPS18_2 (p < 0.0001, ****), VPS39_1 (p < 0.0001, ****), VPS39_2 (p < 0.0001, ****).

negative control and displayed little to no gelatin degradation (Figure 5A, B). We determined cell areas using the cell outline in the actin channel and the nucleus as identifier via DAPI signal. The percentage of degraded area for each cell was calculated by determining the amount of degraded gelatin inside the cell area, indicated by absence of fluorescence, and dividing this by the total cell area. Compared to the WT, the capability to degrade gelatin was reduced in all HOPS KOs, with the VPS39 KOs degrading the least amount of gelatin.

It is important to note the variability of this assay. Factors such as the thickness of the gelatin coating, cell culture, seeding confluency and the amount of incubation time can all greatly influence the observed gelatin degradation. Correct execution of the assay was performed twice (Sup. 3), producing similar results as previously found (Kamphuis, 2020). The data showed a consistent reduced capacity to degrade gelatin for both HOPS KOs, most notably for the VPS39 KOs. This indicates impaired delivery of MT1-MMP and/or other proteases to the cell surface and is consistent with the impaired motility of VPS39 KOs observed earlier.

## HOPS depletion impairs maturation of proteolytic enzymes

To determine whether the impairment in degradative capacity is the result of altered secretion of MT1-MMP, we sought to visualize individual exocytic events of MT1-MMP. To this end, we generated stable cell lines expressing MT1-MMP with a pH sensitive tag: MT1-MMP-pHluorin (Lizárraga et al., 2009). The tag emits green fluorescence at neutral pH, but is quenched in milieus of pH 6 or below. Consequently, it should not fluoresce in acidified compartments such as endosomes or lysosomes. By imaging this construct in combination with LysoTracker, we can observe secretion of MT1-MMP at the plasma membrane from endo-lysosomal compartments in real-time using total internal reflection microscopy (TIRF). Typically, a secretion event should be characterised by the disappearance of LysoTracker signal and concomitant appearance of an MT1-MMP-pHluorin-positive spot (Kajiho et al., 2016). However, we detected spots positive for both LysoTracker and MT1-MMP-pHluorin lingering on the cell surface for up to several minutes before migrating elsewhere in both WT and HOPS KOs (Figure 6A; white arrows). This suggests incomplete fusion of the lysosome with the plasma membrane, which could be facilitated by a

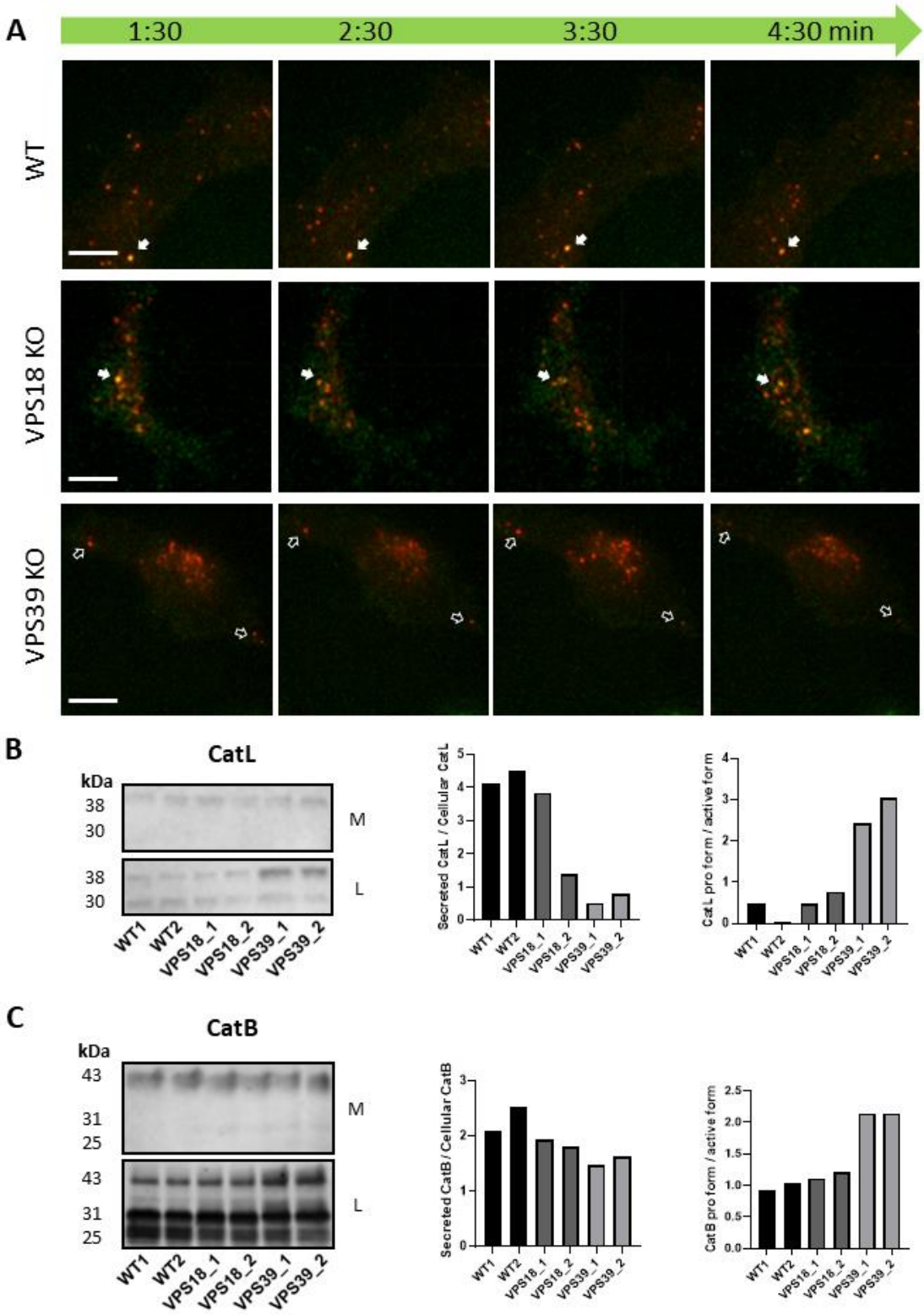


**Figure 6. HOPS depletion impairs maturation of proteolytic enzymes. A.** Total internal reflection microscopy (TIRF) of stable cell lines expressing the pH sensitive MT1-MMP-pHluorin (green) and LysoTracker (red) over 5 min. White arrows indicate stationary lysosomes positive for MT1-MMP-pHluorin. Black arrows indicate accumulation of vesicles in the nuclear and peripheral areas. Scalebar 10 µm. **B.** Western blot of medium (M) and lysate (L) samples stained for CatL. The ratio of secreted CatL over the total cellular fraction and the ratio of pro-CatL (38 kDa) over mature CatL (30 kDa) were quantified and plotted. **C.** Western blot of medium (M) and lysate (L) samples stained for CatB. The ratio of secreted CatL over the total cellular fraction and the ratio of pro-CatB (43 kDa) over mature CatB (31 kDa) were quantified and plotted.

tubular connection, as previously suggested (Figure 1B). We also observed a different distribution of lysosomes in the HOPS KOs: there appeared to be more and smaller vesicles compared to WT conditions. Furthermore, their movement seemed to be more restricted, accumulating either near the nucleus or remaining in the periphery of the cell (Figure 6A; black arrows). Lastly, we observed exocytosis of MT1-MMP in spots that were also LysoTracker-positive (in yellow) in both WT and HOPS KOs. This indicates that there is still recycling of MT1-MMP to the plasma membrane by acidified compartments when HOPS is depleted. Without in depth analysis of exocytic events, it is difficult to assess whether MT1-MMP secretion is altered in the HOPS KOs.

Lastly, we sought to investigate if only secretion of MT1-MMP is affected in HOPS KOs, or if other secreted factors might have an effect on the reduced degradative abilities of these cells. Examination of lysate samples showed that cellular fractions of MT1-MMP were slightly lower in VPS KOs (Sup. 4), but we failed to detect secreted MT1-MMP in the medium. In addition, we stained for other proteases that are secreted at invadopodia to assess whether they contribute to the reduced degradative capacity of HOPS KOs. Staining for Cathepsin L showed that the inactive pro-Cathepsin L (38 kDa) was significantly more abundant than the mature form (30 kDa) in VPS39 KOs (Figure 6B). However, there was a significant decrease in the ratio of secreted cathepsin L over total cellular expression levels (Figure 6B). This indicates a defect in secretion. Cathepsin B showed similar ratios for pro and mature form (Figure 6C), which has also been found for HeLa cells (van der Beek, 2020, unpublished data). It seems the mixed state of endolysosomal compartments in the HOPS depleted cells prevents maturation of these cathepsins. As both cathepsin B and L have been reported to activate pro-uPA, an upstream activator of MT1-MMP, as well as other MMPs (Kazes et al., 1998, Gondi & Rao, 2013), preventing their maturation could decrease activation of MMPs and result in lower degradative capacity in the HOPS KOs.

# Discussion

It has been established that MT1-MMP is a key enzyme in the process of ECM degradation (Sabeh et al., 2004) and that its recycling to invadopodia is necessary to fulfil its degradative functions (Nakahara et al., 1997, Itoh & Seiki, 2004). Kajiho et al. (2016) report that late endosomal trafficking of MT1-MMP involves the HOPS complex, but do not specify how or where this tethering complex is required. To improve our understanding of the degradative pathways involved in cancer metastasis, we sought to elucidate the role of the HOPS complex in MT1-MMP trafficking.

We previously reported less MT1-MMP on the plasma membrane and more in intracellular puncta upon HOPS depletion (Kamphuis, 2020). This accumulation is in line with a defect in late stages of recycling, as opposed to a defect in endocytosis, which leads to higher levels of MT1-MMP on the plasma membrane (Williams & Coppolino, 2011). This highlights the role of HOPS in late endosomal trafficking of MT1-MMP.

In this research, we show that depletion of the HOPS subunits VPS18 and VPS39 results in hybrid early and late endosomal compartments. This is consistent with the phenotype observed in HOPS depleted HeLa cells (van der Beek, 2020, unpublished data) and is likely due to a defect in endolysosomal maturation. As a consequence, MT1-MMP colocalises with a mix of both early endosomal and lysosomal markers. Colocalisation with cathepsin D and LAMP1 was increased in the knockouts, while colocalisation with early endosome marker EEA1 was maintained. Labelling against a panel of endolysosomal markers in immunofluorescence and/or immuno-electron microscopy can elucidate the composition of these mixed compartments in future studies.

Staining for Paxillin showed less pronounced focal adhesion puncta in the HOPS knockouts. This prompted us to investigate whether HOPS depletion resulted in reduced cell motility. While cell track lengths in 2D were similar for wild type and knockouts, cell motility in 3D was shown to be impaired for the VPS39 knockouts. This result is in line with a defect in MT1-MMP localisation to the plasma membrane, as 3D migration requires matrix degradation, while 2D migration does not. The consistency of this assay may be improved by synchronising cell cycles through serum starvation. Fetal Bovine Serum (FBS) contains growth factors and cytokines that may influence cell motility by favouring migration towards higher levels of these substances. Using low levels of FBS (~2%) would therefore result in an assay that is less dependent on external factors. The usage of MMP inhibitor GM6001 could elucidate if the cells only make use of degradational modes of migration, or whether their motility is also influenced by adopting amoeboid morphology. These results could be supported by high magnification imaging of cell morphology in a 3D gel.

The cellular migration results prompted us to look into the degradative abilities of HOPS knockout lines. By gelatin degradation assay, we found that both VPS18 and VPS39 knockouts were impaired in degradation, with VPS39 knockouts more strongly affected. Taken together with the impaired cell motility found for VPS39 knockouts, but not for VPS18 knockouts, this points to a functional difference between these subunits. As mentioned before, VPS18 is also part of the CORVET recycling complex, while VPS39 is specific for the HOPS complex (Balderhaar & Ungermann, 2013). Pryor et al. (2004) reported that HOPS governs heterotypic fusion of late endosomes with a SNARE complex containing VAMP7. VAMP7 in turn is involved in targeting MT1-MMP to invadopodia (Williams et al., 2014). If VAMP7 specifically interacts with VPS39 in late endosomal fusion, this could explain why VPS39 knockouts, and not VPS18 knockouts, are particularly impaired in their degradation capacity. To determine if there is a direct interaction between VAMP7 and VPS39, we propose a binding affinity assay or fluorescence resonance energy transfer (FRET) assay to detect proximity between these proteins.

We wondered if the reduced gelatin degradation in the HOPS depleted cells could be the effect of altered secretion of MT1-MMP. Live cell imaging of HOPS knockout lines stably expressing the pH-sensitive MT1-MMP-pHluorin construct showed colocalisation with lysosomes in both wild type and HOPS knockouts. However, movement of lysosomes in the knockouts appeared restricted, as vesicles would accumulate either at the nucleus or the cell periphery. This may be explained by deregulated maturation of endosomes failing to recruit the appropriate motor proteins for transportation. A possible mechanism that could be disrupted is the recruitment of WASH to late endosomes, either due to absence or incorrect localisation of Retromer or SNX27, which would in

turn prevent interaction with JIP3/4 and dynactin-dynein or kinesin-1 (Monteiro et al., 2013, Marchesin et al., 2015, Sharma et al., 2019). Colocalisation studies of WASH and its interactors in HOPS depleted cells might give more insight into the origin of the mislocalisation of these lysosomes.
We also noted MT1-MMP-pHluorin positive lysosomes lingering on or moving along the plasma membrane. This would imply MT1-MMP 'leaking' from the vesicles or a physical connection between the lysosome and the plasma membrane, such as the tubular structures that Monteiro et al. (2013) observed (Figure 1B). We suggest correlative light and electron microscopy (CLEM), combining live cell imaging of MT1-MMP-pHluorin exocytosis events with structural analysis in EM.
In order to get a deeper understanding of the recycling pathway of MT1-MMP, we recommend using the protein tag HaloTag. This tag is designed to covalently bind to synthetic ligands, enabling real-time detection of MT1-MMP trafficking to specific compartments.
Lastly, we looked into the secretion of other proteolytic enzymes in HOPS knockout lines and found that mature forms of cathepsin B and L were significantly downregulated in VPS39 knockouts. Both cathepsin B and L require localisation to lysosomes to mature (Ishidoh & Kominami, 2002), thus these findings are in line with deregulation of endosomal maturation. This could also provide an explanation for the reduced degradative abilities of these cells, as both cathepsin B and L are upstream regulators of MMPs; they activate urokinase-type plasminogen activator (uPA), that converts plasminogen into plasmin, a potent MMP activator (Murphy et al., 1992, Kazes et al., 1998, Gondi & Rao, 2013). We suggest testing the degradative abilities of HT1080 cells while inhibiting the cathepsin family or their maturation to determine whether results are similar to depletion of HOPS.
MT1-MMP plays a key role in ECM degradation. However, given that invadopodia secrete many different proteases that may also (in)activate each other, it is challenging to find the specific contribution of MT1-MMP to matrix degradation. We have used MMP inhibitor GM6001 in our gelatin degradation assay to reveal that HOPS depletion specifically impairs MMP-mediated degradation in HT1080 cells. Another way to reveal the specific contribution of a protease (family) is the analysis of breakdown products of degraded ECM components. As most families of proteases specialise in degradation of specific ECM components, analysis of breakdown products may reveal more information about the degradation capacity of specific proteases.
Although MT1-MMP accumulates in hybrid compartments in HOPS knockouts, it is still trafficked to the plasma membrane by lysosomes. This is in line with previous work (Pols et al., 2012), in which we reported that VPS39 and VPS41 knockouts were not impaired in their endocytic capacity, but trafficking from late endosomes to lysosomes was delayed. This would also provide an explanation as to why we still detect secretion of Cathepsin B and L in the HOPS knockouts, even though late endosomal and lysosomal maturation are impaired. It is apparent that depletion of HOPS does not abolish late endosomal trafficking.

We have shown that HOPS depletion results in hybrid early and late endosomal compartments and leads to MT1-MMP mislocalisation. Knockout of VPS39 specifically, leads to decreased degradation capacity. These data demonstrate that HOPS depletion affects late endosomal trafficking of MT1-MMP. It is yet unclear which specific molecular interactions govern the trafficking of MT1-MMP from late endosomes to the plasma membrane. On the other hand, it is clear that endosomal trafficking plays an important role in the metastatic capacity of tumour cells. Molecular and cellular studies are required to increase our understanding of the role of endosomal recycling in cancer cell invasion.

# Acknowledgements

I would like to express my gratitude to Prof. Dr. Judtih Klumperman for facilitating my internship at her research group. I would like to extend my sincere thanks to Jan van der Beek for introducing me to the lab, guiding me during my internship as well as providing excellent feedback. I would like to thank Asst. Prof. Nalan Liv for her supervision and her feedback sessions. I would also like to thank Asst. Prof. Antoine Khalil for his expertise on 3D culture assays. I am also grateful to Dr. Valentina Gómez Medallo for her guidance during the lentiviral transduction experiment. Lastly, I'd like to acknowledge my study coordinator, Dr. Martin Harterink, for bringing this internship to my attention.

# Materials and methods

## Cell culture and generation of stable cell lines

HT1080 cells were cultured in T-75 cell culture flasks (Corning) and maintained in a 5% CO2 incubator at 37°C. Cells were grown in DMEM high glucose (Sigma) supplemented with 20% FCS, 100 U/ml penicillin, and 100 µg/ml streptomycin. VPS18 and VPS39 knockouts were made using CRISPR-Cas9 technology, as previously described (Kamphuis, 2020).
Stable H2B-mNeon cell lines were created using the TOL2 transposon system that allows for genome integration. We used a ratio of 2:1 for transposase DNA (D89) : H2B-mNeonGreen x TOL2 (F282). We transfected cells at ~70% confluence using Effectene (Qiagen, 301425). 24 h after transfection, cells were selected using 1 µg/mL Puromycin in DMEM (20% FBS).
The TetOne-MT1-MMP-pHluorin construct was a kind gift from Dr. J. Edgar, Cambridge University. It was cloned into a lentiviral vector (Table 1) to generate cell lines with stable Doxycycline-inducible expression of MT1-MMP-pHluorin through viral transduction. Polybrene was used as a transduction agent. After 48 h, selection was started with 1 µg/mL Puromycin in DMEM (20% FBS).

## Immunofluorescence and colocalisation analysis

Cells were seeded on 12-mm coverslips in a 24-well plate. Cells on coverslips were fixed with 4% FA for 20 minutes followed by 3 washes with PBS and permeabilisation in TritonX-100 0.1% in PBS for 10 minutes. Blocking was performed in 1% BSA in PBS for 10 minutes, after which the coverslips were incubated with primary antibodies in 1% BSA for 1 hour at room temperature (Table 2). Coverslips were incubated with secondary antibodies or phalloidin for 30 minutes at room temperature (Table 3) and mounted in Prolong Diamond (Thermo Fisher Scientific, P36966) with DAPI. Samples were imaged on a Leica Thunder fluorescence microscope using a 100x oil objective. Images were analysed in FIJI using the ComDet 5.5 plugin (Eugene Katrukha, Cell Biology, Utrecht University) and a custom macro.

## Immuno-electron microscopy

TetOne-MT1-MMP-pHluorin expressing cells were grown on 6 cm plates to a confluency of ~80%, then they were fixed with 4% FA in 0.2M Phosphate Buffer (PB) or with 0.2% GA, 4% FA in 0.2M PB. Samples were stored in 0.5% FA at 4°C overnight, after which the fixative was washed off and cells were collected with scrapers in PBS with 1% gelatin. The cells were pelleted, suspended in 12% gelatin at 37°C and then pelleted again, after which the gelatin was solidified on ice. The solidified block was cut into smaller blocks and stored in 2.3M sucrose at 4°C overnight. The blocks were mounted on pins, colour coded and stored in liquid nitrogen. The blocks were cut into thin sections at -100°C using a DiATOME diamond knife in a Leica ultracut cryomicrotome. Sections were subsequently put on carbon-coated grids using a 1:1 mixture of 1.8% methylcellulose and 2.3M sucrose (MCS). Immunolabeling was performed by washing the grids with PBS at 37C to remove the gelatin and MCS. Then, grids were washed 3 times with PBS/0.15% Glycine (20 mM) at RT. Grids were blocked in 1% BSA in PBS for 10 minutes, after which they were incubated for 1 h with primary antibodies in 1% BSA in PBS. The grids were washed three times with 1% BSA in PBS and incubated with Protein-A-Gold (PAG, 10 nm) in 1% BSA in PBS for 30 minutes. Grids were washed 5 times with PBS, fixed with 1% GA in PBS for 5 minutes, and washed with distilled water

10 times. Then they were incubated with 2% Uranyloxalate-acetate PH7 for 5 minutes, and with methyl cellulose uranyl acetate (MC/UA) pH4 on ice for 5-10 minutes. Excess MC/UA was taken off and the grids were dried for 30 minutes before being stored in a grid box. Imaging was performed on a Tecnai T12 TEM using serialEM software. For additional information on sample preparation and immunogold labelling for electron microscopy, see Slot and Geuze (2007).

## Cell migration assay in 2D and 3D

For the 2D migration assay, an 8-wells IBIDI plate was coated with 0.05 mg/mL collagen I in 0.1% acetic acid and dried in a 37°C incubator for 15 minutes, after which the excess was aspirated. Cells were seeded with a confluency of about 20% and left to acclimatise for at least 3h in a 5% CO2 incubator at 37°C before imaging. Slides were imaged on a Leica Thunder wide-field microscope fitted with a live-cell imaging chamber using a 20x air objective. Brightfield for cell morphology and fluorescence imaging of the H2B-mNeon construct were combined. Cells were imaged every 5 minutes for 172 cycles (~14h). Cell tracking was performed in Imaris (version 9.9.1) using the fluorescent nuclei as a guide.

For the 3D migration assay, similarly, an 8-wells IBIDI plate was coated with 0.05 mg/mL collagen I in 0.1% acetic acid and dried in a 37°C incubator for 15 minutes. Meanwhile, a collagen I mixture of 3.78 mg/mL was diluted to a concentration of 1.89 mg/mL, by gently adding 794 µL to a mixture of 150 µL 10x PBS, 9 µL of 1M NaOH and 547 µL of MilliQ. For each well, 15µL of a 500,000 cells/mL solution was added to 150 µL of the collagen I mix, gently mixed and immediately transferred to the preheated, coated IBIDI plate. The collagen I mixture was left to polymerise in a 5% CO2 incubator at 37°C for 40-60 minutes before adding 200µL of medium to the wells. The cells were incubated overnight. Imaging was performed similarly to the 2D migration assay, except this time z-stacks were taken of the region of interest. Cell tracking was performed in Imaris (version 9.9.1) using the fluorescent nuclei as a guide.

## Gelatin degradation assay

Coverslips were cleaned and coated as described by Martin et al. (2012). In short, an unlabelled 5% (w/w) gelatin/sucrose solution was made and kept at 37°C. Meanwhile, 12 mm coverslips were added to a 24-wells plate and cleaned by adding 20% nitric acid for 30 minutes. First, they were washed three times with PBS and coated with 300 µL 50 µg/ml poly-L-lysine left on for 20 minutes before aspiration. Then, after 3 PBS washes, 500 µl of 0.5% freshly made glutaraldehyde was added and coverslips were incubated on ice for 15 minutes. Coverslips were washed 3 times with cold PBS and 500 µl of freshly made 5 mg/ml sodium borohydride (NaBH4) was added for 15 minutes. After 3 additional washes with PBS, Gelatin From Pig Skin, Fluorescein Conjugate (488 nm, Invitrogen, G13187) was added 1:8 to the gelatin stock solution and 100 µL was quickly added to the coverslips and left to dry for 10 minutes. The gelatin was kept shielded from direct light sources as much as possible. After washing three times with PBS and once with 70% ethanol for 30 minutes, the coverslips were kept in PBS in a cold room. Cells were seeded with the aim of roughly 3000 to 6000 cells per coverslip and left to degrade the gelatin layer for 3h in a 5% CO2 incubator at 37°C. Staining with phalloidin for actin and with DAPI was performed as described in the fluorescence and colocalisation section. Samples were imaged on a Leica Thunder fluorescence microscope using a 100x oil objective. Gelatin degradation was quantified in FIJI using a custom macro that determines cell areas using the cell outline in actin and the nucleus as identifier via DAPI

signal. The percentage of degraded area for each cell was calculated by determining the amount of degraded gelatin inside the cell area, indicated by absence of fluorescence, and dividing this by the total cell area. The results were plotted using GraphPadPrism (version 9.3.1).

## Live-cell TIRF imaging

For induction of the TetOne-MT1-MMP-pHluorin construct, we performed a series of dilutions of Doxycyclin and found that a 2 day incubation using a concentration of 1 µg/mL gave robust, medium levels of expression. An 8-wells IBIDI plate was coated with 0.05 mg/mL collagen I in 0.1% acetic acid and left to dry for 15 min in an incubator. The excess solution was aspirated, and medium with 1 µg/mL Doxycyclin was added. Cells were seeded at least 6h before imaging, aiming for 20% to 40% confluency. 15 minutes before imaging, DMEM medium with LysoTracker Red DND-99 (Invitrogen, L7528) was added (1:10000, 1µL in 10mL DMEM). Then, the medium was aspirated and imaging medium was added (Gibco FluoroBrite DMEM, high D-Glucose). TIRF was performed on a Leica Thunder microscope fitted with a live-cell imaging chamber. Sequential dual-colour imaging was done using a 100x oil TIRF objective under an angle of ~67º, resulting in a penetration depth of 82 nm for the 488 nm laser and 94 nm for the 561 nm laser. Exposure was kept at 40 ms. For each condition, three 5-minute videos were recorded, that were subsequently analysed in Imaris (version 9.9.1).

## Immunoblotting

Cells were harvested and lysed in lysis buffer supplemented with 1µM DTT and protease inhibitors. Cell debris was removed by centrifuging at full speed for 15 min at 4°C. Samples of the medium were concentrated using a mini filter column (Sigma Aldrich, UFC501024), in order to enrich for secreted proteins. A Bradford assay was performed to estimate the protein concentration and the samples were subsequently diluted. Sample Buffer (5x) was added and the samples were boiled for 5 minutes before being loaded onto a pre-cast 4-15% gradient gel (Bio-Rad, 4561086). The gels were run for 15 minutes at 60V to clear the stacking gel, then for 30-60 minutes at 100V, after which they were transferred to PVDF membranes (Bio-Rad, 1620174). The membranes were blocked with blocking buffer (2.5mL ODYSSEY Buffer + 2.5mL 1x PBS) for 1 h at room temperature. The primary antibodies were diluted in 2.5mL 1x TBS Tween 0.1% and added to the membranes for overnight incubation (Table 4). Afterwards, the membranes were washed three times with 1x TBS Tween 0.1%, followed by incubation for 1 h with fluorescently labelled secondary antibodies (Table 5) and subsequent washing with PBS and MilliQ. The membranes were imaged on an Amersham Typhoon biomolecular imager.

# Supplements

## Supplement 1

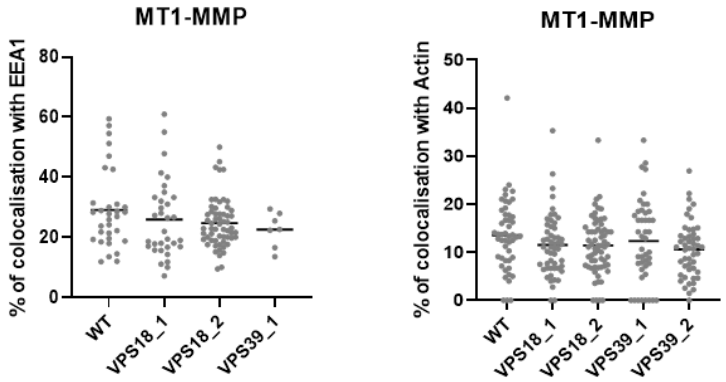


Quantification of the colocalisation of MT1-MMP with EEA1 (left). ANOVA, p = 0.2465, ns. Quantification of the colocalisation of MT1-MMP with actin (right). ANOVA, p = 0.2599, ns.

## Supplement 2

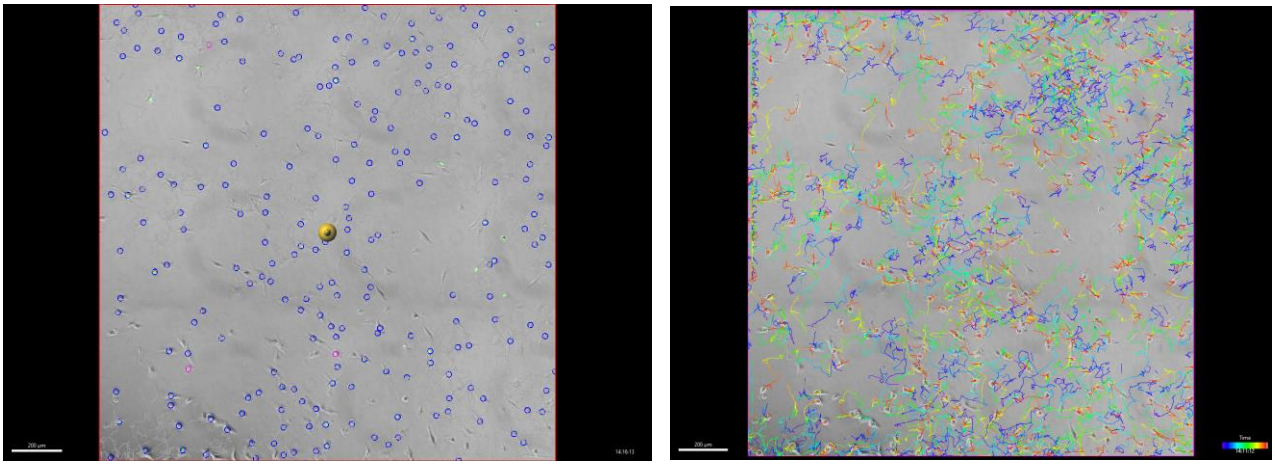

Nuclear tracking of WT and HOPS KOs with H2B-mNeon in Imaris. Detection of nuclei (left). Visualisation of cell tracks (right). Scalebar 200 µm.

# Supplement 3

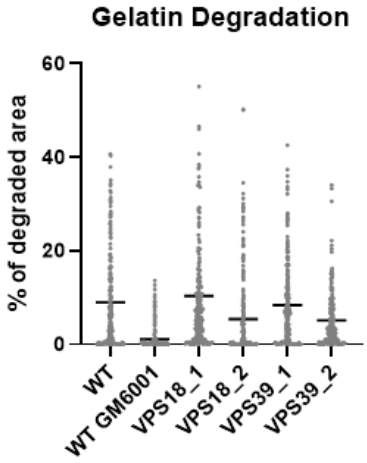


Gelatin degradation assay (N = 2). Quantification of the total percentage of degraded area under each cell (n > 50). Unpaired t-test, VPS18_1 (p = 0.2101, ns), VPS18_2 (p < 0.0001, ****), VPS39_1 (p = 0.4967, ns), VPS39_2 (p < 0.0001, ****).

# Supplement 4

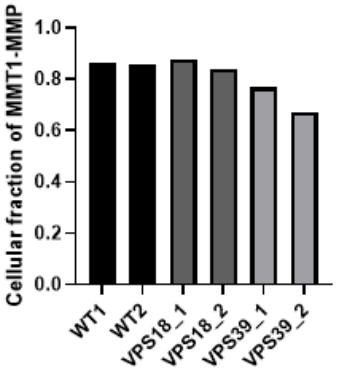


Quantification of immunoblotting of MT1-MMP and actin. The lysate fraction of MT1-MMP was averaged against the lysate fraction of actin.

# Supplement 5

**Table 1.** Primers used for the cloning of TetOne-MT1-MMP-pHluorin into a plasmid with Lentiviral vectors production properties.

| **Primer** | **Sequence** | **Cut sites** |
|---|---|---|
| Forward | AAA**CTGCAG**GCCACAATGTCTCCCGCCCCAAGACC | **PstI** |
| Reverse | AAAGAATTCTTA**GGCGCGCC**TCGGGACCTTGTCCAGCAGGGAAC | EcoRI<br>**AscI** |

# Supplement 6

**Table 2.** Primary antibodies used for immunofluorescence.

| Target | Host species | Catalog number | Dilution |
|---|---|---|---|
| MT1-MMP | Mouse | Millipore (MAB3328-100ug) | 1:200 |
| MT1-MMP | Rabbit | Abcam (ab51074) | 1:100 |
| EEA1 | Rabbit | Cell Signaling (C45B10) | 1:300 |
| Cathepsin D | Goat | RD Systems (AF1014) | 1:500 |
| Paxillin | Mouse | BD biosciences (610052) | 1:500 |

**Table 3.** Secondary antibodies used for immunofluorescence.

| Target | Host species | Emission | Catalog number | Dilution |
|---|---|---|---|---|
| Rabbit | Donkey | 568 nm | Life Technologies (A10042) | 1:250 |
| Goat | Donkey | 647 nm | Life Technologies (A21447) | 1:250 |
| Mouse | Donkey | 488 nm | Life Technologies (A21202) | 1:250 |
| Phalloidin (F-actin) | | 647 nm | Cell Signaling (8940) | 1:50 |

# Supplement 7

**Table 4.** Primary antibodies used for immunoblotting.

| Target | Host species | Catalog number | Dilution |
|---|---|---|---|
| MT1-MMP | Rabbit | Abcam (ab51074) | 1:2000 |
| Actin | Mouse | MP Biomedicals (69100) | 1:20 000 |
| HSP65 | Mouse | Gift from W. van Eden, Utrecht University | 1:1000 |
| Cathepsin B | Goat | RD Systems (AF953) | 1:1000 |
| Cathepsin L | Mouse | BD biosciences (611084) | 1:1000 |

**Table 5.** Secondary antibodies used for immunoblotting.

| Target | Host species | Emission | Catalog number | Dilution |
|---|---|---|---|---|
| Rabbit | Goat | 680 nm | Li-Cor (926-68071) | 1:8000 |
| Goat | Rabbit | 680 nm | Invitrogen (A21088) | 1:8000 |
| Mouse | Goat | 800 nm | Li-Cor (926-32210) | 1:8000 |
| Mouse | Goat | 800 nm | Li-Cor (926-68070) | 1:8000 |

# References


Alberts, B. (2017). *Molecular Biology of the Cell*. Garland Science.

Artym, V. V., Zhang, Y., Seillier-Moiseiwitsch, F., Yamada, K. M., & Mueller, S. C. (2006). Dynamic Interactions of Cortactin and Membrane Type 1 Matrix Metalloproteinase at Invadopodia: Defining the Stages of Invadopodia Formation and Function. *Cancer Research*, *6*, 3034–3043. https://doi.org/10.1158/0008-5472.can-05-2177

Baldassarre, T., Watt, K., Truesdell, P., Meens, J., Schneider, M. M., Sengupta, S. K., & Craig, A. W. (2015). Endophilin A2 Promotes TNBC Cell Invasion and Tumor Metastasis. *Molecular Cancer Research*, *6*, 1044–1055. https://doi.org/10.1158/1541-7786.mcr-14-0573

Balderhaar, H. J. kleine, & Ungermann, C. (2013). CORVET and HOPS tethering complexes**–** coordinators of endosome and lysosome fusion. *Journal of Cell Science*, *6*, 1307–1316. https://doi.org/10.1242/jcs.107805

Bigg, H. F., Morrison, C. J., Butler, G. S., Bogoyevitch, M. A., Wang, Z., Soloway, P. D., & Overall, C. M. (2001). Tissue inhibitor of metalloproteinases-4 inhibits but does not support the activation of gelatinase A via efficient inhibition of membrane type 1-matrix metalloproteinase. *Cancer Research*. (9) 61:3610–3618

Bröcker, C., Kuhlee, A., Gatsogiannis, C., kleine Balderhaar, H. J., Hönscher, C., Engelbrecht-Vandré, S., Ungermann, C., & Raunser, S. (2012). Molecular architecture of the multisubunit homotypic fusion and vacuole protein sorting (HOPS) tethering complex. *Proceedings of the National Academy of Sciences*, *6*, 1991–1996. https://doi.org/10.1073/pnas.1117797109

Burd, C., & Cullen, P. J. (2014). Retromer: A Master Conductor of Endosome Sorting. *Cold Spring Harbor Perspectives in Biology*, *2*, a016774–a016774. https://doi.org/10.1101/cshperspect.a016774

*Cancer*. (2022, February 3). WHO | World Health Organization. https://www.who.int/news-room/fact-sheets/detail/cancer

Carl-McGrath, S., Lendeckel, U., Ebert, M., Roessner, A., & Röcken, C. (2005). The disintegrin-metalloproteinases ADAM9, ADAM12, and ADAM15 are upregulated in gastric cancer. *International Journal of Oncology*. https://doi.org/10.3892/ijo.26.1.17

Cullen, P. J. (2008). Endosomal sorting and signalling: an emerging role for sorting nexins. *Nature Reviews Molecular Cell Biology*, *7*, 574–582. https://doi.org/10.1038/nrm2427

Derivery, E., Sousa, C., Gautier, J. J., Lombard, B., Loew, D., & Gautreau, A. (2009). The Arp2/3 Activator WASH Controls the Fission of Endosomes through a Large Multiprotein Complex. *Developmental Cell*, *5*, 712–723. https://doi.org/10.1016/j.devcel.2009.09.010

D'ortho, M.-P., Will, H., Atkinson, S., Butler, G., Messent, A., Gavrilovic, J., Smith, B., Timpl, R., Zardi, L., & Murphy, G. (1997). Membrane-Type Matrix Metalloproteinases 1 and 2 Exhibit Broad-Spectrum Proteolytic Capacities Comparable to Many Matrix Metalloproteinases. *European Journal of Biochemistry*, *3*, 751–757. https://doi.org/10.1111/j.1432-1033.1997.00751.x

Egeblad, M., & Werb, Z. (2002). New functions for the matrix metalloproteinases in cancer progression. *Nature Reviews Cancer*, *3*, 161–174. https://doi.org/10.1038/nrc745

Ferlay, J., Soerjomataram, I., Dikshit, R., Eser, S., Mathers, C., Rebelo, M., Parkin, D. M., Forman, D., & Bray, F. (2014). Cancer incidence and mortality worldwide: Sources, methods and major patterns in GLOBOCAN 2012. *International Journal of Cancer*, *5*, E359–E386. https://doi.org/10.1002/ijc.29210

Frantz, C., Stewart, K. M., & Weaver, V. M. (2010). The extracellular matrix at a glance. *Journal of Cell Science*, *24*, 4195–4200. https://doi.org/10.1242/jcs.023820

Friedl, P., & Wolf, K. (2003). Tumour-cell invasion and migration: diversity and escape mechanisms. *Nature Reviews Cancer*, *5*, 362–374. https://doi.org/10.1038/nrc1075

Gálvez, B. G., Matías-Román, S., Yáñez-Mó, M., Vicente-Manzanares, M., Sánchez-Madrid, F., & Arroyo, A. G. (2004). Caveolae Are a Novel Pathway for Membrane-Type 1 Matrix Metalloproteinase Traffic in Human Endothelial Cells. *Molecular Biology of the Cell*, *2*, 678–687. https://doi.org/10.1091/mbc.e03-07-0516
Geiger, T. R., & Peeper, D. S. (2009). Metastasis mechanisms. *Biochimica et Biophysica Acta (BBA) - Reviews on Cancer*, *2*, 293–308. https://doi.org/10.1016/j.bbcan.2009.07.006
Gimona, M., Buccione, R., Courtneidge, S. A., & Linder, S. (2008). Assembly and biological role of podosomes and invadopodia. *Current Opinion in Cell Biology*, *2*, 235–241. https://doi.org/10.1016/j.ceb.2008.01.005
Gondi, C. S., & Rao, J. S. (2013). Cathepsin B as a cancer target. *Expert Opinion on Therapeutic Targets*, *3*, 281–291. https://doi.org/10.1517/14728222.2013.740461
Hakulinen, J., Sankkila, L., Sugiyama, N., Lehti, K., & Keski-Oja, J. (2008). Secretion of active membrane type 1 matrix metalloproteinase (MMP-14) into extracellular space in microvesicular exosomes. *Journal of Cellular Biochemistry*, *5*, 1211–1218. https://doi.org/10.1002/jcb.21923
Hanahan, D., & Weinberg, R. A. (2000). The Hallmarks of Cancer. *Cell*, *1*, 57–70. https://doi.org/10.1016/s0092-8674(00)81683-9
Hotary, K. B., Allen, E. D., Brooks, P. C., Datta, N. S., Long, M. W., & Weiss, S. J. (2003). Membrane Type I Matrix Metalloproteinase Usurps Tumor Growth Control Imposed by the Three-Dimensional Extracellular Matrix. *Cell*, *1*, 33–45. https://doi.org/10.1016/s0092-8674(03)00513-0
Huotari, J., & Helenius, A. (2011). Endosome maturation. *The EMBO Journal*, *17*, 3481–3500. https://doi.org/10.1038/emboj.2011.286
Hynes, R. O. (2009). The Extracellular Matrix: Not Just Pretty Fibrils. *Science*, *5957*, 1216–1219. https://doi.org/10.1126/science.1176009
Ishidoh, K., & Kominami, E. (2002). Processing and Activation of Lysosomal Proteinases. *Biological Chemistry*, *12*, 1827–1831. https://doi.org/10.1515/bc.2002.206
Itoh, Y. (2006). MT1-MMP: A key regulator of cell migration in tissue. *IUBMB Life (International Union of Biochemistry and Molecular Biology: Life)*, *10*, 589–596. https://doi.org/10.1080/15216540600962818
Itoh, Y., & Seiki, M. (2004). MT1-MMP: an enzyme with multidimensional regulation. *Trends in Biochemical Sciences*, *6*, 285–289. https://doi.org/10.1016/j.tibs.2004.04.001
Jonker, C. T. H., Galmes, R., Veenendaal, T., ten Brink, C., van der Welle, R. E. N., Liv, N., de Rooij, J., Peden, A. A., van der Sluijs, P., Margadant, C., & Klumperman, J. (2018). Vps3 and Vps8 control integrin trafficking from early to recycling endosomes and regulate integrin-dependent functions. *Nature Communications*, *1*. https://doi.org/10.1038/s41467-018-03226-8
Kajiho, H., Kajiho, Y., Frittoli, E., Confalonieri, S., Bertalot, G., Viale, G., Di Fiore, P. P., Oldani, A., Garre, M., Beznoussenko, G. V., Palamidessi, A., Vecchi, M., Chavrier, P., Perez, F., & Scita, G. (2016). RAB2A controls MT1-MMP endocytic and E-cadherin polarized Golgi trafficking to promote invasive breast cancer programs. *EMBO Reports*, *7*, 1061–1080. https://doi.org/10.15252/embr.201642032
Kazes, I., Delarue, F., Hagège, J., Bouzhir-Sima, L., Rondeau, E., Sraer, J.-D., & Nguyen, G. (1998). Soluble latent membrane-type 1 matrix metalloprotease secreted by human mesangial cells is activated by urokinase. *Kidney International*, *6*, 1976–1984. https://doi.org/10.1046/j.1523-1755.1998.00216.x
Kessenbrock, K., Plaks, V., & Werb, Z. (2010). Matrix Metalloproteinases: Regulators of the Tumor Microenvironment. *Cell*, *1*, 52–67. https://doi.org/10.1016/j.cell.2010.03.015
Knapinska, A. M., & Fields, G. B. (2019). The Expanding Role of MT1-MMP in Cancer Progression. *Pharmaceuticals*, *2*, 77. https://doi.org/10.3390/ph12020077

Knäuper, V., Will, H., López-Otin, C., Smith, B., Atkinson, S. J., Stanton, H., Hembry, R. M., & Murphy, G. (1996). Cellular Mechanisms for Human Procollagenase-3 (MMP-13) Activation. *Journal of Biological Chemistry*, *29*, 17124–17131. https://doi.org/10.1074/jbc.271.29.17124
Koshikawa, N., Giannelli, G., Cirulli, V., Miyazaki, K., & Quaranta, V. (2000). Role of Cell Surface Metalloprotease Mt1-Mmp in Epithelial Cell Migration over Laminin-5. *Journal of Cell Biology*, *3*, 615–624. https://doi.org/10.1083/jcb.148.3.615
Lehti, K., Valtanen, H., Wickström, S., Lohi, J., & Keski-Oja, J. (2000). Regulation of Membrane-type-1 Matrix Metalloproteinase Activity by Its Cytoplasmic Domain. *Journal of Biological Chemistry*, *20*, 15006–15013. https://doi.org/10.1074/jbc.m910220199
Linder, S., Wiesner, C., & Himmel, M. (2011). Degrading Devices: Invadosomes in Proteolytic Cell Invasion. *Annual Review of Cell and Developmental Biology*, *1*, 185–211. https://doi.org/10.1146/annurev-cellbio-092910-154216
Liu, J., Yue, P., Artym, V. V., Mueller, S. C., & Guo, W. (2009). The Role of the Exocyst in Matrix Metalloproteinase Secretion and Actin Dynamics during Tumor Cell Invadopodia Formation. *Molecular Biology of the Cell*, *16*, 3763–3771. https://doi.org/10.1091/mbc.e08-09-0967
Lizárraga, F., Poincloux, R., Romao, M., Montagnac, G., Le Dez, G., Bonne, I., Rigaill, G., Raposo, G., & Chavrier, P. (2009). Diaphanous-Related Formins Are Required for Invadopodia Formation and Invasion of Breast Tumor Cells. *Cancer Research*, *7*, 2792–2800. https://doi.org/10.1158/0008-5472.can-08-3709
Lodillinsky, C., Infante, E., Guichard, A., Chaligné, R., Fuhrmann, L., Cyrta, J., Irondelle, M., Lagoutte, E., Vacher, S., Bonsang-Kitzis, H., Glukhova, M., Reyal, F., Bièche, I., Vincent-Salomon, A., & Chavrier, P. (2015). p63/MT1-MMP axis is required for in situ to invasive transition in basal-like breast cancer. *Oncogene*, *3*, 344–357. https://doi.org/10.1038/onc.2015.87
Lodish, H., Berk, A., Kaiser, C. A., Krieger, M., Bretscher, A., Ploegh, H., Amon, A., & Scott, M. P. (2016). *Molecular Cell Biology*. W. H. Freeman.
Lu, C., Li, X.-Y., Hu, Y., Rowe, R. G., & Weiss, S. J. (2010). MT1-MMP controls human mesenchymal stem cell trafficking and differentiation. *Blood*, *2*, 221–229. https://doi.org/10.1182/blood-2009-06-228494
Luzio, J. P., Parkinson, M. D. J., Gray, S. R., & Bright, N. A. (2009). The delivery of endocytosed cargo to lysosomes. *Biochemical Society Transactions*, *5*, 1019–1021. https://doi.org/10.1042/bst0371019
Macpherson, I. R., Rainero, E., Mitchell, L. E., van den Berghe, P. V., Speirs, C., Dozynkiewicz, M. A., Chaudhary, S., Kalna, G., Edwards, J., Timpson, P., & Norman, J. C. (2014). CLIC3 controls recycling of late endosomal MT1-MMP and dictates invasion and metastasis in breast cancer. *Journal of Cell Science*. https://doi.org/10.1242/jcs.135947
Marchesin, V., Castro-Castro, A., Lodillinsky, C., Castagnino, A., Cyrta, J., Bonsang-Kitzis, H., Fuhrmann, L., Irondelle, M., Infante, E., Montagnac, G., Reyal, F., Vincent-Salomon, A., & Chavrier, P. (2015). ARF6–JIP3/4 regulate endosomal tubules for MT1-MMP exocytosis in cancer invasion. *Journal of Cell Biology*, *2*, 339–358. https://doi.org/10.1083/jcb.201506002
Martin, K. H., Hayes, K. E., Walk, E. L., Ammer, A. G., Markwell, S. M., & Weed, S. A. (2012). Quantitative Measurement of Invadopodia-mediated Extracellular Matrix Proteolysis in Single and Multicellular Contexts. *Journal of Visualized Experiments*, *66*. https://doi.org/10.3791/4119
Meng, N., Li, Y., Zhang, H., & Sun, X.-F. (2008). RECK, a novel matrix metalloproteinase regulator. *Histology and Histopathology*, *23*, 1003–1010. https://doi.org/10.14670/HH-23.1003
Mignatti, P., & Rifkin, D. B. (1993). Biology and biochemistry of proteinases in tumor invasion. *Physiological Reviews*, *1*, 161–195. https://doi.org/10.1152/physrev.1993.73.1.161
Nakahara, H., Howard, L., Thompson, E. W., Sato, H., Seiki, M., Yeh, Y., & Chen, W.-T. (1997). Transmembrane/cytoplasmic domain-mediated membrane type 1-matrix metalloprotease docking to

invadopodia is required for cell invasion. *Proceedings of the National Academy of Sciences*, *15*, 7959–7964. https://doi.org/10.1073/pnas.94.15.7959
Nicolas, J., Magli, S., Rabbachin, L., Sampaolesi, S., Nicotra, F., & Russo, L. (2020). 3D Extracellular Matrix Mimics: Fundamental Concepts and Role of Materials Chemistry to Influence Stem Cell Fate. *Biomacromolecules*, *6*, 1968–1994. https://doi.org/10.1021/acs.biomac.0c00045
Oh, J., Takahashi, R., Kondo, S., Mizoguchi, A., Adachi, E., Sasahara, R. M., Nishimura, S., Imamura, Y., Kitayama, H., Alexander, D. B., Ide, C., Horan, T. P., Arakawa, T., Yoshida, H., Nishikawa, S., Itoh, Y., Seiki, M., Itohara, S., Takahashi, C., & Noda, M. (2001). The Membrane-Anchored MMP Inhibitor RECK Is a Key Regulator of Extracellular Matrix Integrity and Angiogenesis. *Cell*, *6*, 789–800. https://doi.org/10.1016/s0092-8674(01)00597-9
Ohuchi, E., Imai, K., Fujii, Y., Sato, H., Seiki, M., & Okada, Y. (1997). Membrane Type 1 Matrix Metalloproteinase Digests Interstitial Collagens and Other Extracellular Matrix Macromolecules. *Journal of Biological Chemistry*, *4*, 2446–2451. https://doi.org/10.1074/jbc.272.4.2446
Olson, O. C., & Joyce, J. A. (2015). Cysteine cathepsin proteases: regulators of cancer progression and therapeutic response. *Nature Reviews Cancer*, *12*, 712–729. https://doi.org/10.1038/nrc4027
Oser, M., Yamaguchi, H., Mader, C. C., Bravo-Cordero, J. J., Arias, M., Chen, X., DesMarais, V., van Rheenen, J., Koleske, A. J., & Condeelis, J. (2009). Cortactin regulates cofilin and N-WASp activities to control the stages of invadopodium assembly and maturation. *Journal of Cell Biology*, *4*, 571–587. https://doi.org/10.1083/jcb.200812176
Plemel, R. L., Lobingier, B. T., Brett, C. L., Angers, C. G., Nickerson, D. P., Paulsel, A., Sprague, D., & Merz, A. J. (2011). Subunit organization and Rab interactions of Vps-C protein complexes that control endolysosomal membrane traffic. *Molecular Biology of the Cell*, *8*, 1353–1363. https://doi.org/10.1091/mbc.e10-03-0260
Pols, M. S., ten Brink, C., Gosavi, P., Oorschot, V., & Klumperman, J. (2012). The HOPS Proteins hVps41 and hVps39 Are Required for Homotypic and Heterotypic Late Endosome Fusion. *Traffic*, *2*, 219–232. https://doi.org/10.1111/tra.12027
Pols, M. S., van Meel, E., Oorschot, V., ten Brink, C., Fukuda, M., Swetha, M. G., Mayor, S., & Klumperman, J. (2013). hVps41 and VAMP7 function in direct TGN to late endosome transport of lysosomal membrane proteins. *Nature Communications*, *1*. https://doi.org/10.1038/ncomms2360
Poteryaev, D., Datta, S., Ackema, K., Zerial, M., & Spang, A. (2010). Identification of the Switch in Early-to-Late Endosome Transition. *Cell*, *3*, 497–508. https://doi.org/10.1016/j.cell.2010.03.011
Pryor, P. R., Mullock, B. M., Bright, N. A., Lindsay, M. R., Gray, S. R., Richardson, S. C. W., Stewart, A., James, D. E., Piper, R. C., & Luzio, J. P. (2004). Combinatorial SNARE complexes with VAMP7 or VAMP8 define different late endocytic fusion events. *EMBO Reports*, *6*, 590–595. https://doi.org/10.1038/sj.embor.7400150
Redondo-Muñoz, J., Escobar-Díaz, E., Samaniego, R., Terol, M. J., García-Marco, J. A., & García-Pardo, A. (2006). MMP-9 in B-cell chronic lymphocytic leukemia is up-regulated by α4β1 integrin or CXCR4 engagement via distinct signaling pathways, localizes to podosomes, and is involved in cell invasion and migration. *Blood*, *9*, 3143–3151. https://doi.org/10.1182/blood-2006-03-007294
Remacle, A., Murphy, G., & Roghi, C. (2003). Membrane type I-matrix metalloproteinase (MT1-MMP) is internalised by two different pathways and is recycled to the cell surface. *Journal of Cell Science*, *19*, 3905–3916. https://doi.org/10.1242/jcs.00710
Ricard-Blum, S. (2010). The Collagen Family. *Cold Spring Harbor Perspectives in Biology*, *1*, a004978–a004978. https://doi.org/10.1101/cshperspect.a004978
Rink, J., Ghigo, E., Kalaidzidis, Y., & Zerial, M. (2005). Rab Conversion as a Mechanism of Progression from Early to Late Endosomes. *Cell*, *5*, 735–749. https://doi.org/10.1016/j.cell.2005.06.043

Rossé, C., Lodillinsky, C., Fuhrmann, L., Nourieh, M., Monteiro, P., Irondelle, M., Lagoutte, E., Vacher, S., Waharte, F., Paul-Gilloteaux, P., Romao, M., Sengmanivong, L., Linch, M., van Lint, J., Raposo, G., Vincent-Salomon, A., Bièche, I., Parker, P. J., & Chavrier, P. (2014). Control of MT1-MMP transport by atypical PKC during breast-cancer progression. *Proceedings of the National Academy of Sciences*, *18*. https://doi.org/10.1073/pnas.1400749111
Rozario, T., & DeSimone, D. W. (2010). The extracellular matrix in development and morphogenesis: A dynamic view. *Developmental Biology*, *1*, 126–140. https://doi.org/10.1016/j.ydbio.2009.10.026
Sabeh, F., Ota, I., Holmbeck, K., Birkedal-Hansen, H., Soloway, P., Balbin, M., Lopez-Otin, C., Shapiro, S., Inada, M., Krane, S., Allen, E., Chung, D., & Weiss, S. J. (2004). Tumor cell traffic through the extracellular matrix is controlled by the membrane-anchored collagenase MT1-MMP. *Journal of Cell Biology*, *4*, 769–781. https://doi.org/10.1083/jcb.200408028
Sabeh, F., Shimizu-Hirota, R., & Weiss, S. J. (2009). Protease-dependent versus -independent cancer cell invasion programs: three-dimensional amoeboid movement revisited. *Journal of Cell Biology*, *1*, 11–19. https://doi.org/10.1083/jcb.200807195
Sato, H., Takino, T., Okada, Y., Cao, J., Shinagawa, A., Yamamoto, E., & Seiki, M. (1994). A matrix metalloproteinase expressed on the surface of invasive tumour cells. *Nature*, *6484*, 61–65. https://doi.org/10.1038/370061a0
Seaman, M. N. J., Gautreau, A., & Billadeau, D. D. (2013). Retromer-mediated endosomal protein sorting: all WASHed up! *Trends in Cell Biology*, *11*, 522–528. https://doi.org/10.1016/j.tcb.2013.04.010
Segala, G., Bennesch, M. A., Ghahhari, N. M., Pandey, D. P., Echeverria, P. C., Karch, F., Maeda, R. K., & Picard, D. (2019). Vps11 and Vps18 of Vps-C membrane traffic complexes are E3 ubiquitin ligases and fine-tune signalling. *Nature Communications*, *1*. https://doi.org/10.1038/s41467-019-09800-y
Seiki, M. (2003). Membrane-type 1 matrix metalloproteinase: a key enzyme for tumor invasion. *Cancer Letters*, *1*, 1–11. https://doi.org/10.1016/s0304-3835(02)00699-7
Seyfried, T. N., & Huysentruyt, L. C. (2013). On the Origin of Cancer Metastasis. *Critical Reviews™ in Oncogenesis*, *1–2*, 43–73. https://doi.org/10.1615/critrevoncog.v18.i1-2.40
Sharma, P., Parveen, S., Shah, L. V., Mukherjee, M., Kalaidzidis, Y., Kozielski, A. J., Rosato, R., Chang, J. C., & Datta, S. (2019). SNX27–retromer assembly recycles MT1-MMP to invadopodia and promotes breast cancer metastasis. *Journal of Cell Biology*, *1*. https://doi.org/10.1083/jcb.201812098
Slot, J. W., & Geuze, H. J. (2007). Cryosectioning and immunolabeling. *Nature Protocols*, *10*, 2480–2491. https://doi.org/10.1038/nprot.2007.365
Solinger, J. A., & Spang, A. (2013). Tethering complexes in the endocytic pathway: CORVET and HOPS. *FEBS Journal*, *12*, 2743–2757. https://doi.org/10.1111/febs.12151
Sounni, N. E., Devy, L., Hajitou, A., Frankenne, F., Munaut, C., Gilles, C., Deroanne, C., Thompson, E. W., Foidart, J. M., & Noel, A. (2002). MT1-MMP expression promotes tumor growth and angiogenesis through an up-regulation of vascular endothelial growth factor expression. *The FASEB Journal*, *6*, 555–564. https://doi.org/10.1096/fj.01-0790com
Sporn, M. B. (1996). The war on cancer. *The Lancet*, *9012*, 1377–1381. https://doi.org/10.1016/s0140-6736(96)91015-6
Steffen, A., Le Dez, G., Poincloux, R., Recchi, C., Nassoy, P., Rottner, K., Galli, T., & Chavrier, P. (2008). MT1-MMP-Dependent Invasion Is Regulated by TI-VAMP/VAMP7. *Current Biology*, *12*, 926–931. https://doi.org/10.1016/j.cub.2008.05.044

Stetler-Stevenson, W. G., Aznavoorian, S., & Liotta, L. A. (1993). Tumor Cell Interactions with the Extracellular Matrix During Invasion and Metastasis. *Annual Review of Cell Biology*, *1*, 541–573. https://doi.org/10.1146/annurev.cb.09.110193.002545
Tanabe, L. M., & List, K. (2016). The role of type II transmembrane serine protease-mediated signaling in cancer. *The FEBS Journal*, *10*, 1421–1436. https://doi.org/10.1111/febs.13971
Temkin, P., Lauffer, B., Jäger, S., Cimermancic, P., Krogan, N. J., & von Zastrow, M. (2011). SNX27 mediates retromer tubule entry and endosome-to-plasma membrane trafficking of signalling receptors. *Nature Cell Biology*, *6*, 715–721. https://doi.org/10.1038/ncb2252
Uekita, T., Itoh, Y., Yana, I., Ohno, H., & Seiki, M. (2001). Cytoplasmic tail–dependent internalization of membrane-type 1 matrix metalloproteinase is important for its invasion-promoting activity. *Journal of Cell Biology*, *7*, 1345–1356. https://doi.org/10.1083/jcb.200108112
Ullrich, O., Reinsch, S., Urbé, S., Zerial, M., & Parton, R. G. (1996). Rab11 regulates recycling through the pericentriolar recycling endosome. *Journal of Cell Biology*, *4*, 913–924. https://doi.org/10.1083/jcb.135.4.913
van der Kant, R., Jonker, C. T. H., Wijdeven, R. H., Bakker, J., Janssen, L., Klumperman, J., & Neefjes, J. (2015). Characterization of the Mammalian CORVET and HOPS Complexes and Their Modular Restructuring for Endosome Specificity. *Journal of Biological Chemistry*, *51*, 30280–30290. https://doi.org/10.1074/jbc.m115.688440
Will, H., Atkinson, S. J., Butler, G. S., Smith, B., & Murphy, G. (1996). The Soluble Catalytic Domain of Membrane Type 1 Matrix Metalloproteinase Cleaves the Propeptide of Progelatinase A and Initiates Autoproteolytic Activation. *Journal of Biological Chemistry*, *29*, 17119–17123. https://doi.org/10.1074/jbc.271.29.17119
Williams, K C, & Coppolino, M. G. (2011). Phosphorylation of membrane type 1-matrix metalloproteinase (MT1-MMP) and its vesicle-associated membrane protein 7 (VAMP7)-dependent trafficking facilitate cell invasion and migration. *Journal of Biological Chemistry, 286, 43405–43416*. https://doi.org/https://doi.org/10.1074/jbc.M111.297069
Williams, Karla C., McNeilly, R. E., & Coppolino, M. G. (2014). SNAP23, Syntaxin4, and vesicle-associated membrane protein 7 (VAMP7) mediate trafficking of membrane type 1–matrix metalloproteinase (MT1-MMP) during invadopodium formation and tumor cell invasion. *Molecular Biology of the Cell*, *13*, 2061–2070. https://doi.org/10.1091/mbc.e13-10-0582
Wolf, K., Wu, Y. I., Liu, Y., Geiger, J., Tam, E., Overall, C., Stack, M. S., & Friedl, P. (2007). Multi-step pericellular proteolysis controls the transition from individual to collective cancer cell invasion. *Nature Cell Biology*, *8*, 893–904. https://doi.org/10.1038/ncb1616
Wyckoff, J. B., Pinner, S. E., Gschmeissner, S., Condeelis, J. S., & Sahai, E. (2006). ROCK- and Myosin-Dependent Matrix Deformation Enables Protease-Independent Tumor-Cell Invasion In Vivo. *Current Biology*, *15*, 1515–1523. https://doi.org/10.1016/j.cub.2006.05.065
Yamaguchi, H., Lorenz, M., Kempiak, S., Sarmiento, C., Coniglio, S., Symons, M., Segall, J., Eddy, R., Miki, H., Takenawa, T., & Condeelis, J. (2005). Molecular mechanisms of invadopodium formation. *Journal of Cell Biology*, *3*, 441–452. https://doi.org/10.1083/jcb.200407076
Yu, X., Zech, T., McDonald, L., Gonzalez, E. G., Li, A., Macpherson, I., Schwarz, J. P., Spence, H., Futó, K., Timpson, P., Nixon, C., Ma, Y., Anton, I. M., Visegrády, B., Insall, R. H., Oien, K., Blyth, K., Norman, J. C., & Machesky, L. M. (2012). N-WASP coordinates the delivery and F-actin–mediated capture of MT1-MMP at invasive pseudopods. *Journal of Cell Biology*, *3*, 527–544. https://doi.org/10.1083/jcb.201203025